

## Quantifying Uncertainty in Geothermal Reservoir Modeling

Christian Vogt<sup>1</sup>, Darius Mottaghay<sup>2</sup>, Volker Rath<sup>1,4</sup>, Andreas Wolf<sup>3</sup>, Renate Pechnig<sup>2</sup> and Christoph Clauser<sup>1</sup>

<sup>1</sup>Applied Geophysics and Geothermal Energy, E.ON Energy Research Center, RWTH Aachen University, Aachen, Germany

<sup>2</sup>Geophysica Beratungsgesellschaft mbH, Aachen, Germany

<sup>3</sup>Scientific Computing, RWTH Aachen University, Aachen, Germany

<sup>4</sup>Departamento de Física de la Tierra, Astronomía y Astrofísica II, Universidad Complutense de Madrid, Spain

cvogt@eonerc.rwth-aachen.de

**Keywords:** Failure Risk; Performance Forecasting; Sequential Gaussian Simulation; Monte Carlo; Probability distributions; Thermal Conductivity; Heat Flow.

### ABSTRACT

An increased use of geothermal energy requires reliable estimates of the risk of failure and the project cost. These estimates can be provided by quantifying the uncertainty of subsurface rock properties and state variables, such as temperature or pressure, in a geothermal reservoir.

This quantification can be obtained by using a stochastic approach called Monte Carlo simulation. To this end, we integrated the stochastic algorithm "Sequential Gaussian Simulation" *Sgsim* into our in-house mass and heat flow simulator *Shemat\_suite*. *Sgsim* generates an ensemble of parameter realizations for the same geometrical reservoir model, where each realization corresponds equally likely to the real situation defined by data. By providing this ensemble of realizations, the stochastic approach allows us not only to obtain average values and error estimates of a target rock property or state variable at any location in the geothermal reservoir but also their local probability distribution.

As a demonstration of this method, an exploration scenario is simulated for a projected geothermal district heat use in The Hague, Netherlands.

### 1. INTRODUCTION

An increased use of geothermal energy requires a reliable estimate of the risk of failure with respect to the exploration and development of geothermal reservoirs. Suitable geothermal reservoirs need to satisfy certain characteristics for an economic production of geothermal heat. The likelihood of fulfilling these requirements defines the risk. For instance, the generation of electrical power with geothermal steam requires a minimum flow rate of  $50 \text{ L s}^{-1}$  -  $100 \text{ L s}^{-1}$  and a temperature of  $150 \text{ }^{\circ}\text{C}$  -  $200 \text{ }^{\circ}\text{C}$  (e.g. Clauser 2006). Consequently, the entire geothermal system needs to be characterized as precisely as possible. The numerical simulation of the geothermal system and the processes acting within play a crucial role in all stages of the exploration, development, and operation of any given reservoir. The prediction uncertainty of the numerical simulation and the risk estimate depend on the uncertainties associated with different reservoir parameters. These are, in particular, the subsurface rock properties, such as thermal and hydraulic conductivities, and the state variables in a geothermal reservoir, such as temperature and pressure.

Uncertainties can be quantified and minimized based on a stochastic approach provided by various geostatistical

algorithms presented by Caers (2005) and Chiles & Delfiner (1999). Various software tools for geostatistical estimation of rock properties are available (Remy 2005; Anonymous A 1996). They are based on the widely-used geostatistical software library GSLIB (Deutsch & Journel 1998). These tools yield distributions of spatial rock properties. State variables must be predicted by a corresponding heat and fluid flow simulation (e.g., Clauser 2003; Xu et al. 2004; Anonymous B 2001). Finsterle & Kowalsky (2007) describe an approach which combines stochastic methods and flow simulation. This comprises inverse modeling (Tarantola 2004) and forecasting geostatistical parameters such as correlation lengths. However, this approach does not allow the stochastic simulation of boundary conditions. Geostatistical algorithms were already applied successfully in research in hydrogeology (Nowack 2005; Cooley 2004; Kitanidis 1997), repositories for nuclear waste (Neuman & Wierenga 2002) and hydrocarbon reservoir characterization (Li et al. 2008; Campos 2002). In geothermal reservoir characterization however, geostatistical algorithms have rarely been used although they are promising for uncertainty quantification and hence risk estimation. Uncertainty estimation based on Monte Carlo techniques is described by Robert & Casella (2004); Monte Carlo simulation for predicting hydrocarbon reservoir performance is reported by Abhulimen & Otubu (2007).

In the stochastic approach elaborated in this paper - a Monte Carlo study - multiple parameter realizations of the same geometrical reservoir model are generated. Each realization is equally likely to correspond to the real situation defined by data. The reservoir state variables are predicted from simulations of fluid flow and heat transport for each realization. This yields not only average values and error estimates of a target rock property or state variable at any location in the geothermal reservoir, but also their local probability distribution. Both the geostatistical and the flow simulation are performed within one software tool. This also comprises parallelization to distribute a large number of realizations over several processor cores. Additionally, the approach allows the stochastic simulation of boundary conditions.

As a rule, geothermal reservoirs are usually explored only by few boreholes as compared to hydrocarbon reservoirs. Therefore, additional information is required in order to constrain the stochastic results and hence, to minimize the uncertainty further. By post-processing of the modeling results using a constraining method, information from state variable measurements is added. By applying the method presented in this paper, state variables obtained from forward transport simulations, such as temperature or tracer concentration, are compared with available data such as

bottom-hole temperatures. By comparison, realizations corresponding to an unsatisfactory data fit are discarded.

Therefore, the overall work flow comprises a conditioning of the realization ensemble to rock properties (geostatistical algorithms) and state variables (constraining method). Based on this information, the risk within a geothermal project can be estimated more accurately. As a result, cost may be reduced and estimated with less uncertainty.

To demonstrate this approach and its advantages, an exploration scenario is simulated for a current geothermal district heating project in The Hague, Netherlands (Anonymous C 2006). In this steady-state exploration scenario, we focus on thermal rock properties. In future studies, hydraulic properties will play an important role in simulating the operation phase of this project or in other scenarios where advective heat transport is significant. Additionally, the stochastic modeling of boundary conditions is also applied to this field study.

## 2. METHOD AND NUMERICAL SIMULATION

By computing fluid flow and heat transport, state variables of a reservoir can be obtained from the spatial distribution of subsurface rock properties and boundary conditions, such as basal specific heat flow. The stochastic approach - a Monte Carlo study - is based on modifying these rock properties. Thus, the simulation work flow is subdivided into different parts: (i) the stochastic part, Sequential Gaussian Simulation; (ii) the flow simulation by forward modeling; (iii) a constraining post-processing.

### 2.1 Sequential Gaussian Simulation

For a set of chosen geological units, ensembles of realizations for a target rock property are generated using the stochastic algorithm "Sequential Gaussian Simulation" *Sgsim* from the Geostatistical Software Library GSLIB (Deutsch & Journel 1998). *Sgsim* uses a Kriging interpolation technique for spatially distributed data (e.g., Deutsch & Journel 1998). Kriging stands for a family of least-square regression methods yielding optimal estimates of the target parameters.

For each grid node, Kriging returns a mean value, the Kriging mean, and an average squared error called Kriging semi-variance for each node. By approximating the semi-variogram by a weighting of the available data, Kriging accounts for the underlying data correlation. The semi-variogram represents a measure for the dissimilarity of spatial data as a function of the distance between pairs of data (Deutsch & Journel 1998).

The *Sgsim* algorithm operates as follows:

- (i) The geometry of a geothermal reservoir model is discretized on a specific grid.
- (ii) All data is transformed into gaussian shape with mean equals zero and variance equals one.
- (iii) The algorithm follows a random path through the model.
- (iv) For each grid node, nearby data and already simulated nodes are used for a Kriging of the target property
- (v) A property value drawn randomly from the distribution defined by Kriging mean and variance is assigned to the node. Consequently, these values take into account (a) assumed or measured property distributions; (b) the

correlation length; (c) primary data, such as borehole measurements; (d) secondary data, such as seismic data.

- (vi) A realization is completed when property values are assigned to all nodes of the model.
- (vii) The model is transformed back from gaussian into the original space.
- (viii) More realizations are created by following other random paths. Each of these realizations is equally likely with respect to the real situation defined by data (Figure 1).

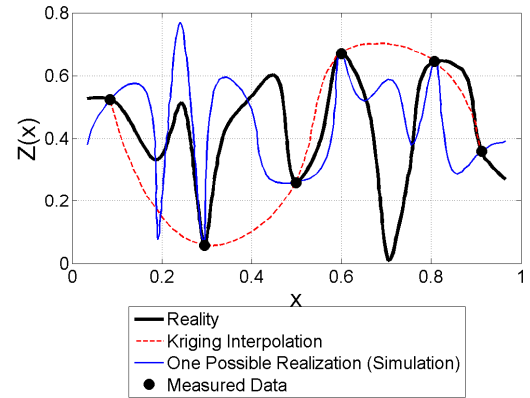


**Figure 1: 1D example for a geostatistical parameter estimation showing the Kriging interpolation technique and a realization generated with *Sgsim* (after Schafmeister 1999).**

The *Sgsim* algorithm is integrated as a module into the fluid flow and heat transport simulator *Shemat\_suite*. This way, the generated realizations can be used directly as input for the fluid and heat transport simulations, wasting no time and effort for format conversion. Further, already existing models implemented in the flow simulator can be easily updated with a stochastic simulation. Additionally, the module represents the initial step of a strategy for iterative improvement of an ensemble of information forming a geothermal reservoir model. This ensemble will be updated as different kinds of observations, such as logging data, well tests, or even tracer experiments become available. This iterative process will be implemented using various numerical tools, such as ensemble Kalman filters (Gu & Oliver 2006) or genetic algorithms (Romero & Carter 2001).

### 2.1 Constraining Method

Using a constraining method, state variables are used to find appropriate realizations of an ensemble characterized by different spatial distributions of rock properties. This benefits directly from the coupled modeling work flow with respect to rock properties and forward modeling of the fluid flow and heat transport. Realizations which fail to fit the measured state variables, e.g. temperature, sufficiently well at certain locations in the model are discarded from the ensemble.

For larger changes of the temperature field as expected in the presence of significant fluid flow, constraining post-processing is more effective when applied to hydraulic rather than to thermal properties. This has been demonstrated in previous studies on synthetic models done by us which will be published soon and are not presented in this paper.

### 3. FIELD STUDY FOR A GEOTHERMAL RESERVOIR

A geothermal district heating project in The Hague, Netherlands, (Anonymous C 2006) is chosen to demonstrate the stochastic work flow as outlined above. The temperature in the target area is predicted, and its uncertainty is minimized. A geothermal doublet will be installed at a depth of 2200 m to supply up to 6000 households with geothermal heat. The Delft sandstone at the transition between Jurassic and Cretaceous formations is identified as target reservoir. Its permeability there is roughly  $10^{-11} \text{ m}^2$ . Expected temperature and flow rate are 75 °C and  $42 \text{ L s}^{-1}$ , respectively. Model parameters such as reservoir geometry and basal specific heat flow of  $65 \text{ mW m}^{-2}$  are reported by Simmink & Vandewijer (2008). Rock properties such as thermal conductivity and heat production rate are calculated from seismic wave velocity, gamma ray and neutron density measured logging data from a calibration borehole. As an example, Fig. 2 shows logs for dry and saturated thermal conductivity obtained from inversions of these logs done by us on a similar set of data. Consistent with available geological information available (Simmink & Vandewijer 2008), there is neither significant thermal free convection nor topological driven fluid flow. Thus, conductive heat flow dominants. The temperature prediction is obtained from a steady-state simulation of fluid flow and heat transport. For comparison of model and reality, ten corrected bottom-hole temperatures (BHT) are available distributed evenly in the study area. The modeling process aims for a temperature prediction at the proposed target location near the center of the model.

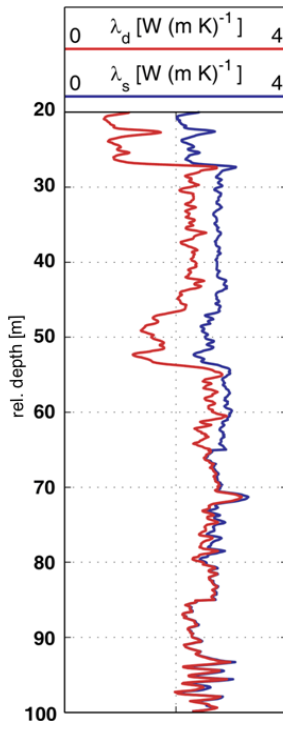


**Figure 2: Example for dry and saturated thermal conductivity ( $\lambda_d$  and  $\lambda_s$ ) obtained from inversions of seismic velocity, gamma ray, and neutron density logs.**

The 3D geometric model (Mottaghy et al. 2009; Pechnig et al. 2008) represents a volume of  $22.5 \text{ km} \times 24.3 \text{ km} \times 5 \text{ km}$ . It is discretized into  $150 \times 162 \times 100$  grid cells. It comprises nine geological layers identified and implemented as separate units. A first estimate for the possible range in the

predicted temperature is obtained by characterizing each unit by its mean and standard deviation of the thermal conductivity according to the geometric modeling process. In particular, a temperature range is obtained by using on the one hand always minimum values (mean - standard deviation) and on the other hand always maximum values (mean + standard deviation) of the thermal conductivity in each layer for the modeling.

The result of the prediction at the positions of the BHT data is illustrated in Fig. 3. According to Förster (2001), even single corrected BHT values usually underestimate the formation temperature by 8 K with a standard deviation of  $\pm 8 \text{ K}$ . Thus, 8 K is added to each BHT value. Obviously, the mean reproduces every single BHT successfully, but the uncertainty is over-estimated. More information about the reliability of corrected BHT data and its error is given in Hermanrud 1990 and Deming 1989.

#### 3.1 Quantifying and Reducing Uncertainty

The stochastic work flow explained in section 2 is applied to provide a better uncertainty estimates. Instead of considering only minimum and maximum values defined by mean and standard deviation, the original probability distribution of the saturated thermal conductivity in the calibration borehole is simulated in six of the nine geological units using the *Sgsim* algorithm. As an example for the different input histograms to be reproduced using *Sgsim*, the measured distributions of the Layer 3 (Lower Cretaceous Supergroup) and Layer 4 (Jurassic Supergroup) are illustrated in Fig. 4. The original distributions are calculated by us using different logs (Fig. 2), as stated above.

With 10 boreholes in an area of about  $550 \text{ km}^2$ , the borehole density is quite low, so that unconditioned *Sgsim* has to be performed. This can be done without restricting the results as our previous tests of the *Sgsim* algorithm done on a synthetic model did show. Therefore, one calibration borehole with high vertical data density is sufficient for our stochastic simulation. However, the logs in the other boreholes indicate the same stratigraphy.

Correlation lengths in the vertical direction are calculated using the semi-variogram (see section 2.1). The data required for the semi-variograms are obtained from the calibration borehole. The semi-variograms yield correlation lengths between 50 m and 450 m for the individual geological layers.

Due to the nature of sedimentation, there is an anisotropy between the vertical and horizontal correlation lengths (Caers 2005). Vertical correlation lengths usually are much shorter than horizontal ones. For the horizontal directions, the low borehole density is insufficient to calculate reliable semi-variograms. Fortunately, the horizontal direction is less important for the predominantly vertical conductive heat flow. However, to obtain a maximum variance in the ensemble of realizations, large correlation lengths are implemented in the horizontal directions by multiplying the corresponding vertical correlation length in each unit. Deutsch & Journel (1998) use a maximum factor of 16 between vertical and horizontal correlation length which is adopted in this study, too. This yields horizontal correlation lengths between 800 m and 7200 m. However, these values can be considered as more or less arbitrary due to the dominantly vertical direction of heat flow. Nevertheless, simulating fluid flow in the reservoir, e.g. for performance prediction during the operation of the doublet, will require reasonable values in the future.

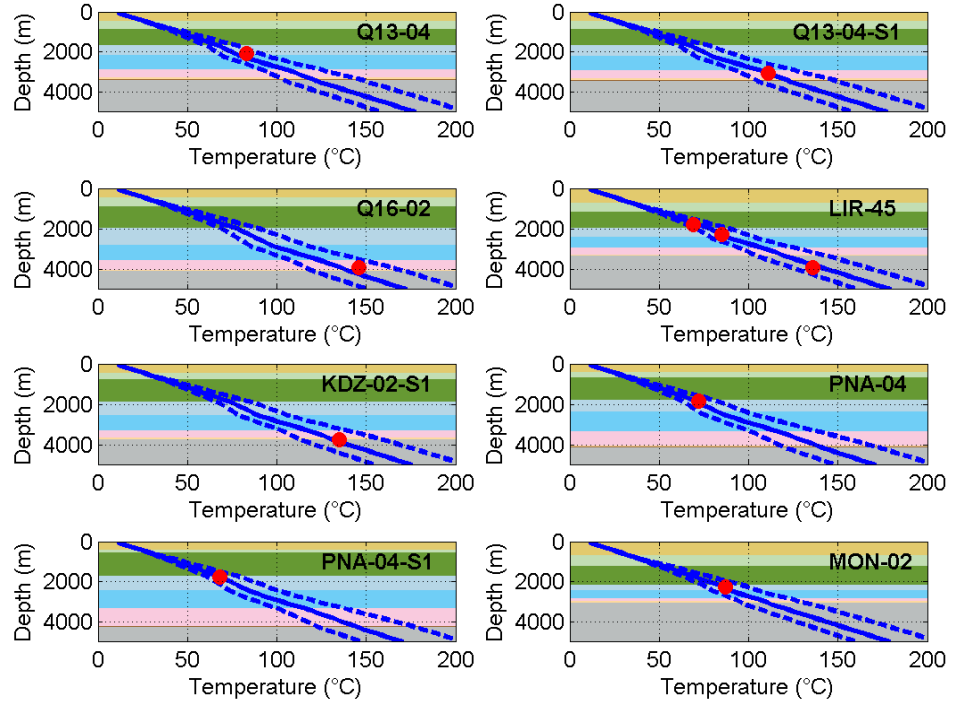


**Figure 3: Temperature prediction (blue line) at the positions of the BHT and BHT values (red dots) as well as uncertainty estimate (blue dashed line).**

1000 temperature fields are simulated based on 1000 realizations of thermal conductivity in the model. One example is shown in Fig. 6. Constraining post-processing discards unsuitable ensemble realizations in order to reduce the uncertainty further

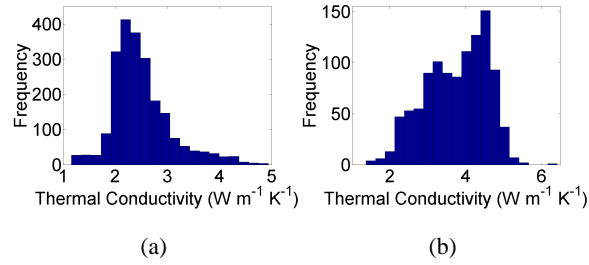


**Figure 4: Original distributions of the thermal conductivity in the Lower Cretaceous Supergroup (a) and the Jurassic Supergroup (b) obtained from our inversions of logging data.**

### 3.2 Constraining post-processing

Constraining methods are useful to further reduce the uncertainty significantly. Therefore, we perform the constraining post-processing in this case, too, although constraining techniques are supposed to be less effective in systems lacking significant fluid flow, as stated above. In this post-processing, the temperatures of all 1000 realizations of the ensemble are compared to the measured BHT. The underestimation of corrected BHT is  $8 \text{ K} \pm 8 \text{ K}$  (Förster 2001), as mentioned above. Thus, 8 K is added again and a standard deviation of  $\pm 8 \text{ K}$  as a constraining parameter for the post-processing. A

realization is discarded from the ensemble, if the difference between the temperature simulated at the position of the BHT measurement and the BHT value exceeds  $\pm 8 \text{ K}$  for at least one BHT.

The probability distribution of the temperature at the proposed target location is shown for 1000 original realizations in Fig. 5(a) and for the 235 realizations which survived the constraining post-processing in Fig. 5(b). The full distribution width of the temperature is reduced from 18 K to 13 K as a consequence of the post-processing. In particular, realizations with high temperature predictions are removed from the ensemble and the distribution mean of  $87 \text{ }^{\circ}\text{C}$  is reduced by 1 K. Thus, overly optimistic assumptions suggested by the stochastic work flow without constraining the ensemble are avoided.

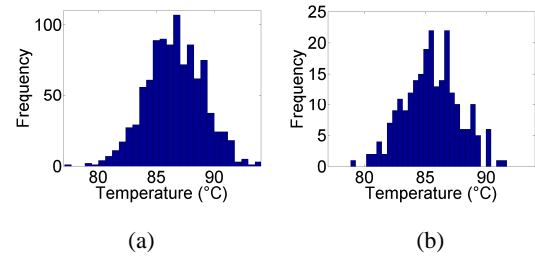


**Figure 5: Temperature at proposed target location (a) for the original ensemble and (b) for the ensemble after constraining post-processing (b). In (b), the uncertainty is further reduced.**

As in Fig. 3, the result of the temperature predictions at the locations of the BHT is illustrated in Fig. 7 for the 235

realizations. Again, 8 K is added to each BHT. The BHT are reproduced with an appropriate uncertainty.

Overall, the final temperature prediction obtained the 235 surviving realizations is illustrated in Fig. 8 in comparison with the initial uncertainty. Obviously, the uncertainty has been minimized significantly by applying the work flow. The full distribution width is reduced from 26 K to 13 K,

making the temperature prediction much more accurate. In addition, not only the full distribution width, but also a standard deviation of 2.3 K is yielded assuming a Gaussian distribution shape. As further positive result in terms of project feasibility, the minimum predicted temperature exceeds the projected temperature of 75 °C for each realization.

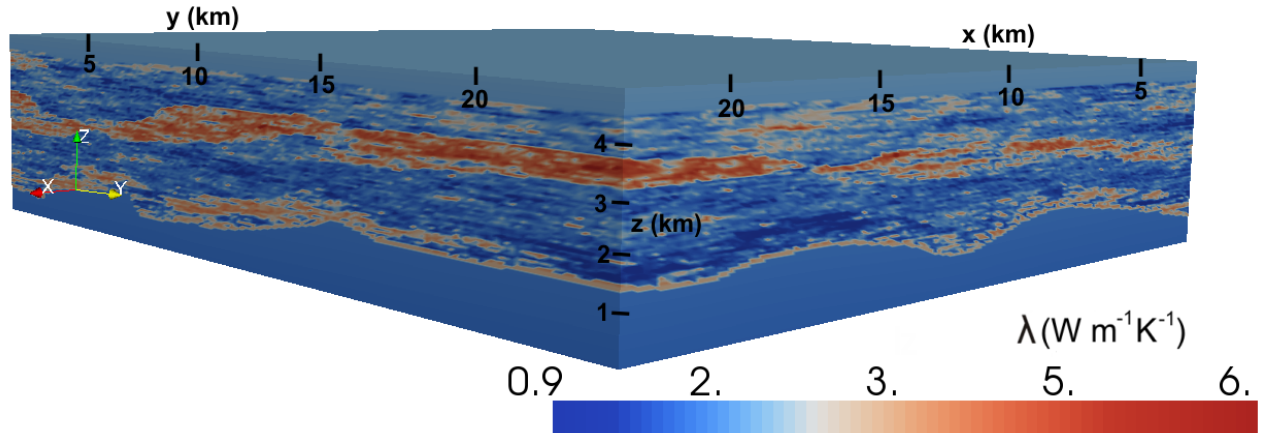


Figure 6: One realization of the thermal conductivity in the model.

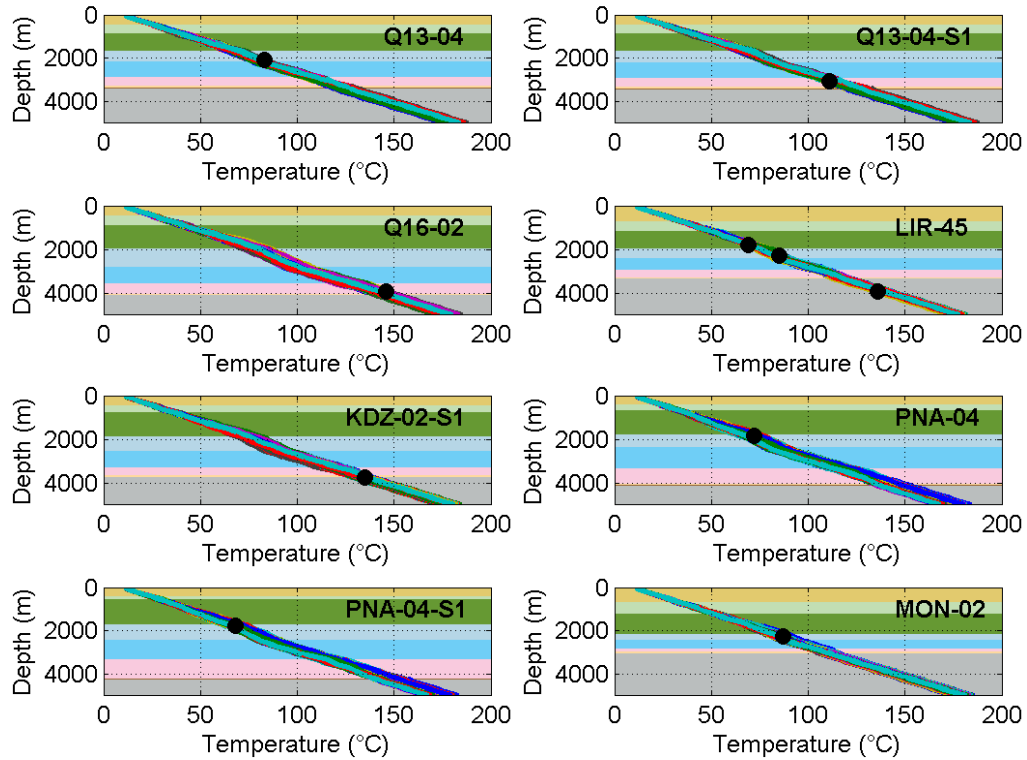
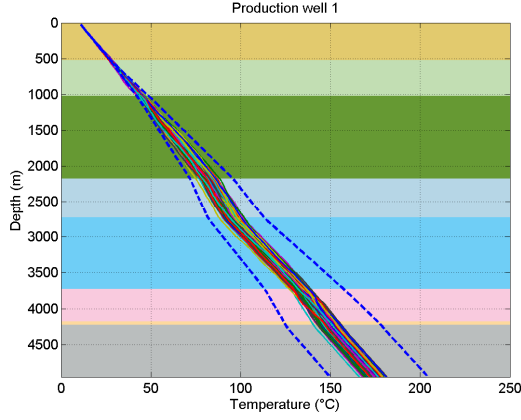


Figure 7: Temperature prediction (colored lines) at the positions of the BHT and BHT values (black dots) after applying Monte Carlo post-processing in comparison with the original uncertainty estimate (blue dashed line)



**Figure 8: Temperature prediction (colored lines) at proposed target location in comparison to the original uncertainty estimate (blue dashed line).**

#### 4. ADDITIONAL STOCHASTIC SIMULATION OF BASAL SPECIFIC HEAT FLOW

Taking advantage of the possibility for stochastic modeling of boundary conditions, an additional stochastic simulation of the basal specific heat flow is integrated in the work flow in order to consider this major factor of uncertainty in the modeling process. The mean of  $q = 65 \text{ mW m}^{-2}$  is varied with a standard deviation of  $\pm 3 \text{ mW m}^{-2}$ . The simulated value is assigned to each grid node at the bottom boundary of the model. Again, an ensemble of 1000 realizations is generated.

According to Lee et al. (1996), a typical standard deviation of the basal heat flow is  $\pm 20 \text{ \%}$ , which corresponds to  $\pm 13 \text{ mW m}^{-2}$  in this case. But due to the good agreement of the final corrected BHT with the predicted temperatures obtained from the simulated realizations illustrated in Fig. 3, less fluctuation of the basal specific heat flow is assumed. Moreover, the need of a statistically relevant amount of realizations surviving the constraining selection demands this smaller value of  $\pm 3 \text{ mW m}^{-2}$ .

Now, with an expected larger distribution width due to basal specific heat flow fluctuation, constraining post-processing is essential to identify reliable realizations. The results of the complete stochastic work flow including boundary simulation are illustrated in Fig. 9 and Fig. 10. Before performing constraining post-processing, the increased uncertainty caused by including the basal specific heat flow results in a decreased minimum temperature of about  $75 \text{ °C}$ . Interestingly, this minimum temperature equals the projected temperature of  $75 \text{ °C}$  for each realization, even when the basal specific heat flow is varied.

As expected, the full distribution width without constraining post-processing increases significantly from  $18 \text{ K}$  to  $27 \text{ K}$  at target depth compared to the distribution discussed in section 3.1. The mean of  $87 \text{ °C}$  does not change, but the standard deviation increases to  $4.5 \text{ K}$ . The fraction of realizations which survived the constraining post-processing decreases from  $235 / 1000$  to  $138 / 1000$  due to the wider distribution. However, the distribution characteristics, a mean of  $86 \text{ °C}$  and a standard deviation of  $2.3 \text{ K}$ , after performing the constraining post-processing are actually identical to the characteristics in section 3.2. The full distribution width of about  $11 \text{ K}$  after performing the constraining method is actually lower than for a constant basal specific heat flow. This is due to the smaller size of the statistical sample.

A varying basal specific heat flow is not considered for the original uncertainty estimate without any stochastic approach. Nevertheless, the temperature profiles of all realizations fall into the estimated original range. In this particular case, constraining post-processing reduces significantly the large effects on the uncertainty estimate by simulating basal specific heat flow. Thus, uncertainty estimates obtained with and without stochastic basal specific heat flow simulation yield similar results. Although the system is not dominated by fluid flow and thus no hydraulic properties are simulated, the Monte Carlo approach combined with constraining post-processing proves very efficient in this case of stochastic simulation of thermal rock properties and boundary conditions.

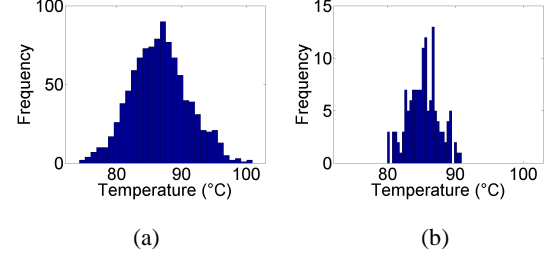


**Figure 9: Temperature at proposed target location (a) for the original ensemble and (b) for the ensemble after constraining post-processing including a stochastically simulated basal specific heat flow.**

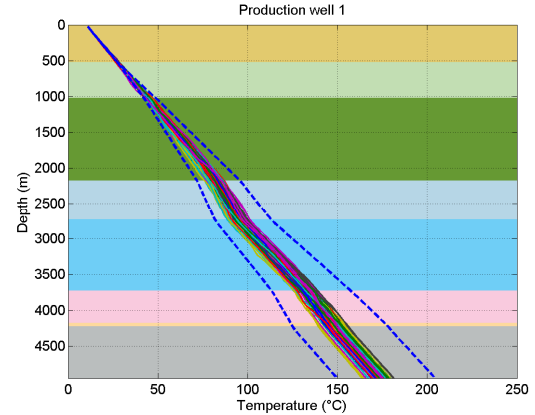


**Figure 10: Temperature prediction (colored lines) at proposed target location in comparison to the original uncertainty estimate (blue dashed line). Here, basal specific heat flow is additionally simulated stochastically. Note that the original uncertainty estimate is based on an average value for the basal specific heat flow.**

#### 5. CONCULSIONS

Geothermal reservoir exploration and modeling requires sophisticated quantification of uncertainty. The Monte Carlo approach of Sequential Gaussian Simulation combined with constraining post-processing helps to quantify and reduce significantly the uncertainty in the prediction of state variables in geothermal reservoirs. Multiple realizations are generated conditioned to measured rock properties and therefore equally likely to reflect reality. They are combined with conditioning to measured state variables via constraining post-processing. Thus, uncertainty is quantified stochastically much more precisely than basing merely on a minimum-maximum estimate of the involved rock properties. Hence, it is very effective in reducing

uncertainties and thus in reducing cost. Additionally, the stochastic simulation of boundary conditions allows a more comprehensive approach to quantify uncertainty in geothermal reservoirs.

Constraining techniques are particularly effective in filtering realizations after stochastic simulation of hydraulic properties, which has to be demonstrated in other field studies. Thus, stochastic permeability modeling is planned for transient simulations of the operated geothermal doublet in The Hague. In particular, this will predict the temperature development at the target location and the propagation of the cold water front from the injection point. The possibility to establish different grid sizes for the stochastic and the flow simulation will then be utilized. As soon as first measurements of the state variables become available after drilling, a constraining approach in a fluid flow dominated temperature field will be performed.

Furthermore, an optimal visualization of an ensemble of realization and their uncertainty in 2D and 3D projection in cooperation with experts for virtual reality environments is in progress (Wieskopf & Erlebacher 2004; Wolter et al. 2009).

Monte Carlo and conditioning methods, especially for transient simulations and hydraulic properties will be supplemented by sophisticated methods such as ensemble Kalman filters (Gu & Oliver 2006) or genetic algorithms (Romero & Carter 2001).

The content of this paper is connected to other papers published during this conference: Koch et al. (2010) describe the development of a statistical rock property data base; Clauser et al. (2010) present the joint MeProRisk – Project which aims at developing a toolbox for iterative improvement of reservoir models.

## ACKNOWLEDGMENTS

Our research was funded by the the German Federal Ministry for the Environment, Nature Conservation and Nuclear Safety (BMU), grant FKZ 0327563, and by the German Ministry of Education and Science (BMBF), grant 03SF0326A. We thank IF Technology (Arnhem, Netherlands) and TNO Built Environment and Geosciences (Delft, Netherlands) for providing data and granting permission to publish results, as well as Eneco Energy (Rotterdam, Netherlands) and E.ON Benelux (Rotterdam, Netherlands) for initiating and funding the districted heating project in The Hague, from which these data are derived.

## REFERENCES

Abhulimen, K. E., and Otubu, O. A.: Predicting Reservoir Performance Using Stochastic Monte Carlo Simulation, *E-Journal Of Reservoir Engineering*, **1**(1), (2007), <http://petroleumjournalsonline.com/journals/index.php/reservoir>.

Anonymous A: GOCAD User's Manual, Association Scientifique pour la Geologie et ses Applications, Ecole Nationale Supérieure de Geologie, Nancy, (1996).

Anonymous B: Eclipse-100, Technical Description Manual, Schlumberger GeoQuest, Houston TX, (2001).

Anonymous C: <http://www.denhaag.com/default.asp?id=7096&ep=>, (2006)

Caers, J.: Petroleum Geostatistics, Society of Petroleum Engineers, Richardson TX (2005).

Campos, O. M.: Spatial Distribution Of Calcite Concretions Inferred From Borehole Image Data And Their Use In Reservoir Modeling: An Application To Breitbrunn Field, *Master's thesis*, The University of Texas, Austin TX, (2002).

Chiles, J. P., and Delfiner, P.: Geostatistics: Modeling Spatial Uncertainty, *Wiley & Sons*, New York, (1999).

Clauser, C. (ed): Numerical Simulation of Reactive Flow in Hot Aquifers. *SHEMAT* and processing *SHEMAT*, *Springer*, Heidelberg-Berlin, (2003).

Clauser, C.: Geothermal Energy, in Landolt-Börnstein, GroupVIII "Advanced Material and Technologies", Vol. 3 "Energy Technologies", Subvol. C "Renewable Energies", ed. Heinloth, K., *Springer Verlag*, Heidelberg-Berlin, (2006), 480–595.

Clauser, C. et al.: MeProRisk – a Tool Box for Evaluating and Reducing Risks in Exploration, Development, and Operation of Geothermal Reservoirs, *Proceedings*, World Geothermal Congress 2010, Bali, Indonesia, (2010)

Cooley, R. L.: A theory for modeling ground-water flow in heterogeneous media, *Professional Paper* 1679, U.S. Geological Survey (USGS), Reston VA, (2004).

Deming, D.: Application of Botton-hole temperature corrections in, geothermal studies, *Geothermics*, **18**(5/6), (1989), 775–786.

Deutsch, C. V., and Journel, A. G.: *GSLIB*. Geostatistical software library and user's guide, *Oxford University Press*, New York, (1998).

Diersch, H. J.-G., and Kolditz, O.: Variable-density flow and transport in porous media: Approaches and challenges, *Advances in Water Resources*, **25**, (2002), 899–944.

Finsterle, S. & Kowalsky, M. B.: iTOUGH2-GSLIB Users Guide, Earth Sciences Division, Lawrence Berkeley National Laboratory, University of California, Berkeley CA (2007).

Förster, A.: Analysis of borehole temperature data in the Northeast German Basin: continuous logs versus bottom-hole temperatures, *Petroleum Geoscience*, **7**(3), (2001), 241–254.

Gosselin, L., Tye-Gingras, M., and Mathieu-Potvin, F.: Review of utilization of genetic algorithms in heat transfer problems, *International Journal of Heat and Mass Transfer*, **52**, (2009), 2169–2188.

Gu, Y., and Oliver, D. S.: The ensemble Kalman filter for continuous updating of reservoir simulation models, *Journal of Energy Resources Technology*, **128**(87), (2006).

Hermanrud, C., Cao, S., and Lerche, I.: Estimates of virgin rock temperature derived from BHT measurements: Bias and error, *Geophysics*, **55**(7), (1990), 924–931.

Kitanidis, P. K.: Introduction to Geostatistics, Applications in Hydrogeology, *Cambridge University Press*, Cambridge, (1997).

Koch A., Jorand R., Vogt C., Pechnig R., and Clauser C.: Statistically Based Physical Rock Properties for Improved Geothermal Reservoir Models with Quantified Uncertainty, *Proceedings*, World Geothermal Congress 2010, Bali, Indonesia, (2010)

Kolditz, O., Ratke, R., Diersch, H.-J. G., and Zielke, W.: Coupled groundwater flow and transport: 1.

Verification of variable density flow and transport models, *Advances in Water Resources*, **21**, (1998), 21–46.

Lee, Y., Deming, D., and Chen, K.: Heat flow and heat production in the Arkoma Basin and Oklahoma Platform, southeastern Oklahoma, *Journal of Geophysical Research*, **101**(B11), (1996), 25,387–25,401.

Li, S., Zhang, C., Yin, Y., Yin, T., and Yan, S.: Stochastic modeling of reservoir with multi-source, *Earth Science Frontiers*, **15**(1), (2008), 196–201.

Mottaghy, D., Pechnig, R., Willemsen, G., and Simmelink, E.: Geothermal Project Den Haag – 3-D models for temperature prediction and reservoir characterization, *European Geoscience Union General Assembly EGU2009*, Vienna, (2009), <http://meetingorganizer.copernicus.org/EGU2009/EGU2009-11862.pdf>

Neuman, S. P., and Wierenga, P. J.: A comprehensive strategy of hydrogeologic modeling and uncertainty analysis for nuclear facilities and sites, *Tech. Rep. NUREG/CR8605*, University of Arizona for U. S. Nuclear Regulatory Commission, Office of Nuclear Regulatory Research, Washington DC, (2002).

Nowack, W.: Geostatistical methods for the identification of flow and transport parameters in the subsurface, Doctoral dissertation, Institut für Wasserbau, Universität Stuttgart, (2005).

Pechnig, R., Mottaghy, D., Willemsen, G., and Simmelink, H. J.: The Den Haag geothermal district heating project – 3-d models for temperature prediction, *Schriftenreihe der Deutschen Gesellschaft für Geowissenschaften*, **60**, (2008), 309, <http://www.dgg.de/pub/schriftenreihe>.

Remy, N.: S-GeMS: The Stanford Geostatistical Modeling Software: A tool for new algorithms development, in *Geostatistics Banff 2004*, eds Leuangthong, O. and Deutsch, C. V., *Springer*, Dordrecht, (2005).

Robert, C. P., and Casella, G.: Monte Carlo statistical methods, *Springer*, New York, (2004).

Romero, C., and Carter, J.: Using genetic algorithms for reservoir characterisation, *Journal of Petroleum Science and Engineering*, **31**, (2001), 113–123.

Schafmeister, M.-T.: *Geostatistik für die hydrogeologische Praxis*, *Springer-Verlag*, Berlin Heidelberg, (1999).

Simmelink, H. J., and Vandeweijer, V.: *Geothermie Den Haag Zuid-West, 2e fase geologisch onderzoek*, *Tech. Rep 034.72157.*, Netherlands Organisation for Applied Natural Science Research (TNO) , Utrecht, (2008).

Tarantola, A.: Inverse problem theory. Methods for model parameter estimation, *Society for Industrial and Applied Mathematics (SIAM)*, Philadelphia PA, (2004).

Wieskopf, D., and Erlebacher, G.: The Visualization Handbook, In *Overview of Flow Visualization*, Elsevier Academic Press, (2004), 261–278.

Wolter, M., Tedjo-Palczynski, I., Hentschel, B., and Kuhlen, T.: Spatial Input for Time Navigation in Scientific Visualizations, *IEEE Computer Graphics and Applications*, (2009), submitted.

Xu, T., Sonnenthal, E., Spycher, N., and Pruess, K.: TOUGHREACT Users Guide: A Simulation Program for Non-isothermal Multiphase Reactive Geochemical Transport in Variably Saturated Geologic Media, Lawrence Berkeley National Laboratory Report LBNL-55460, Berkeley CA. (2004).